

## Optical and Dielectric Properties of $Mn^{2+}$ & $Co^{2+}$ : $B_2O_3$ -ZnO-MgO Glasses

M. Venkateswarlu<sup>1,2\*</sup>, B.H. Rudramadevi<sup>2</sup> and S.Buddhudu<sup>2</sup>

<sup>1</sup>Department of Physics, Sri Ramakrishna Degree & P.G. (Autonomous) College, Nandyal-518 501, India

<sup>2</sup>Department of Physics, Sri Venkateswara University, Tirupati-517 502, India

**Abstract:** A transparent base glass in the chemical composition  $B_2O_3$ -ZnO-MgO (BZM) has successfully been prepared and a couple of transition metal ( $Mn^{2+}$  &  $Co^{2+}$ ) ions doped into this glass matrix have also been done for their further analysis. Optical absorption, photoluminescence (excitation & emission) spectra, dielectric ( $\epsilon'$  and  $\tan \delta$ ) and ac conductivity measurements have been undertaken for  $Mn^{2+}$  &  $Co^{2+}$ :  $B_2O_3$ -ZnO-MgO. The visible absorption spectrum of  $Mn^{2+}$ : BZM glass has shown a broad absorption band at 456 nm ( ${}^6A_{1g}(S) \rightarrow {}^4T_{1g}(G)$ ), whereas three bands at 526 nm ( ${}^4T_{1g}(F) \rightarrow {}^2T_{1g}(H)$ ), at 584 nm ( ${}^4A_2({}^4F) \rightarrow {}^4T_1({}^4P)$ ) and at 1429 nm ( ${}^4A_2({}^4F) \rightarrow {}^4T_1({}^4F)$ ) are observed from  $Co^{2+}$ : BZM optical glass. The nature of local symmetry and structural information of the neighboring atoms of dopant ions ( $Mn^{2+}$  &  $Co^{2+}$ ) in the host matrix have been understood by evaluating the crystal field strength (Dq) and Racah (B & C) parameters. The emission spectrum of  $Mn^{2+}$ : BZM glass exhibits a single and broad emission band at 616 nm and it is assigned to a spin forbidden transition of  ${}^4T_{1g}({}^4G) \rightarrow {}^6A_{1g}({}^6S)$  with an excitation  $\lambda_{exc} = 414$  nm. While in the case of  $Co^{2+}$ : BZM glass a single emission band at 640 nm and it is assigned to a spin forbidden transition of  ${}^4T_1({}^4P) \rightarrow {}^4A_2({}^4F)$  with an excitation  $\lambda_{exc} = 580$  nm has been observed. The frequency dependence of dielectric parameters ( $\epsilon'$  and  $\tan \delta$ ) and ac conductivity in the frequency range 1 Hz to 2 MHz at room temperature for these glasses have been studied. The low frequency dispersion in the profiles of dielectric constant and loss tangent would be resulting in because of space charge polarization effect at the electrode-electrolyte interface and it is also noticed that  $\sigma_{ac}$  increases in accordance with frequency change.

**Keywords:**  $Mn^{2+}$  and  $Co^{2+}$  glasses, Spectral analysis, Dielectric properties, ac conductivity

### I. Introduction

In recent years, there has been a considerable interest in the study of glasses doped with transition metal ions because of their potential applications as lasers, photo-conductive devices, magnetic materials, especially for tunable solid state lasers, efficient phosphors, etc.[1-4].  $B_2O_3$  is one of the best glass formers known and is present in almost all commercially important glasses. It is often used as dielectric and insulating material and it is known that borate glass is a good shield against infrared radiation [5]. Borate glasses are used as electro-optic modulators, electro-optic switches, solid-state laser materials and non-linear optical parametric converters [6]. Borate glasses doped with certain transition metal ions have been studied by several researchers [7-14]. When alkaline-earth cations incorporated in the structure of borate glasses, glass transition temperature increases, strength of the glass structure could be increased and chemical resistance of the glass may be raised [15]. It has also been noticed that the presence of ZnO content in the glassy matrices, stability of the material becomes stronger, with a high thermal resistance against the crystallization [16]. Transition metal ions are incorporated in to these glasses in order to characterize their optical, dielectric and conductivity behaviors. Glasses containing transition metal ions have become the subject of interest owing to their potential applications.

Among the various transition metal ions, manganese ion is particularly interesting because it exists in different valence states with different coordination different glass matrices [17], for example as  $Mn^{3+}$  in borate glasses with octahedral coordination whereas in silicate and germanate glasses it exists in  $Mn^{2+}$  with both octahedral and tetrahedral coordination [18-20]. Among different manganese ions,  $Mn^{2+}$  and  $Mn^{3+}$  are well known paramagnetic ions and  $Mn^{2+}$  and  $Mn^{4+}$  are identified as luminescence activators. In  $Mn^{2+}$ , its spectral position can vary from green to deep red color, depending on coordination and ligand field strength. Usually, tetrahedral coordination ( ${}^{IV}Mn^{2+}$ , weak crystal field) results in green emission whereas octahedral coordination ( ${}^{VI}Mn^{2+}$ , stronger crystal field) results in orange to red emission [21]

Another important transition metal ion is cobalt. Cobalt ion is very interesting because of its two stable valence states viz.,  $Co^{2+}$  and  $Co^{3+}$  with tetrahedral and octahedral coordinations in glass network and exhibits d-d transitions due to optical excitation.  $Co^{2+}$  ion produces a thick blue color in glasses and its color shade changes with the transformation of its tetrahedral coordination to octahedral or vice-versa depending on the concentration of CoO, experimental conditions and nature of the host glass system. CoO doped glasses are

significantly important in the materials technology in terms of optical switching devices, visible and near infrared laser materials, ferromagnetic sensors, etc. The cobalt ions exhibit a strong absorption band in the near infrared region (1.3- 1.6  $\mu m$ ) due to  $^4A_{2g}(^4F) \rightarrow ^4T_{1g}(^4F)$  transition in the glass matrices [22]; in view of this the cobalt containing glasses are being used as NIR laser materials. The study of dielectric properties, such as dielectric constant, loss factor, and ac conductivity over a wide range of frequency help in assessing the insulating character of the glasses but also throw some light on the structural aspects of these glasses [23].

In the present work, we have reported and discussed the absorption, excitation and emission spectra of the above given transition metal ions ( $Mn^{2+}$  &  $Co^{2+}$ ) in BZM glass system and also discussed the variation of dielectric parameter and ac conductivity over a wider range of frequency.

## II. Experimental Studies

### 2.1. Glass Samples Preparation

Glasses studied in the present work were prepared by a standard melt quenching technique. The chemical compositions (all are in mol %) of the host (reference) glass with and without transition metal ions as dopants are as follows:

- $65B_2O_3$ - $20ZnO$ - $15MgO$  : BZM (host glass)
- $64.5B_2O_3$ - $20ZnO$ - $15MgO$ - $0.5MnO_2$  :  $Mn^{2+}$ :BZM
- $64.8B_2O_3$ - $20ZnO$ - $15MgO$ - $0.5CoCl_2$  :  $Co^{2+}$ :BZM

The starting chemicals were used in analytical grade such as  $H_3BO_3$ ,  $ZnCO_3$ ,  $MgCO_3$ ,  $MnO_2$ , and  $CoCl_2 \cdot 6H_2O$ . All the chemicals were weighed in 10g batch each separately, thoroughly mixed using an agate mortar and a pestle and then each of those was collected into porcelain crucible and heated in an electric furnace for melting them for an hour at  $980^\circ C$ . Melt mixture was repeatedly stirred to ensure a total homogenization. This melt was then quenched in between two smooth surfaced brass plates; bubble free glasses in circular designs having 2–3 cm in diameters and a thickness of 0.3 cm were obtained. Due to the homogeneous distribution of transition metal ions in the glass matrices, these bubble free transparent glasses have displayed brighter colours as shown in Fig. 1.  $Mn^{2+}$ : BZM glass has exhibited brown colour and  $Co^{2+}$ : BZM glass has demonstrated blue colour and a colourless host glass.

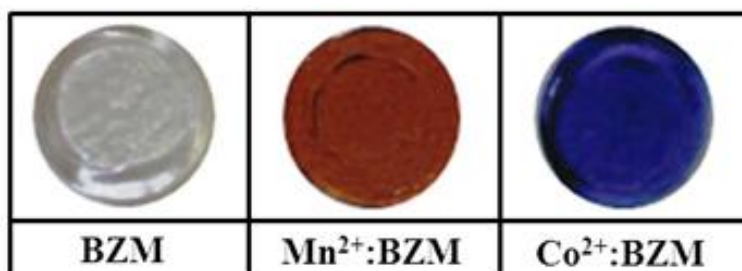


Figure 1. Photographs of reference BZM,  $Mn^{2+}$ : BZM &  $Co^{2+}$ : BZM glasses

### 2.2. Measurements

The optical absorption spectra of BZM glasses doped with certain transition metal ions ( $Mn^{2+}$  &  $Co^{2+}$ ) were recorded at room temperature in the spectral range of 250 nm- 2500nm on a Varian-Cary-Win spectrometer (JASCO V-570). Excitation & emission spectra were recorded at room temperature on a SPEX Fluorolog-3 (Model-II) spectrophotometer, attached with a Xe-arc lamp (450 W) as the excitation source. Electrical conductivity measurements were carried using a two electrode cell configuration by sandwiching the glass samples between brass electrodes at room temperature over a frequency range of 1 Hz – 2 MHz at an ac voltage strength of  $0.5 V_{rms}$  on a Phase Sensitive Multimeter (PSM 1700) in LCR mode for acquiring the data of real and imaginary parts of complex impedance. The calculation of conductivity ( $\sigma_{ac}$ ), real ( $\epsilon'$ ) and imaginary ( $\epsilon''$ ) parts of dielectric constant ( $\epsilon^*$ ), dielectric loss ( $\tan \delta$ ) were performed using raw impedance data based on the capacitance, sample dimensions and electrode area.

## III. Theoretical Analysis

**Manganese:** The ground-state electron configuration of  $Mn^{2+}$  is written as  $A(3d)^5$ , where A stands for the completed argon shell with eighteen electrons. In a cubic crystalline field of low to moderate strength, these five d electrons of  $Mn^{2+}$  ion are distributed in  $t_{2g}$  and  $e_g$  orbitals, with three in the former and two in the later. Thus, the ground state configuration is written as  $(t_{2g})^3$  and  $(e_g)^2$ . This configuration gives rise to the electronic states,  $^6A_{1g}$ ,  $^4A_{1g}$ ,  $^4E_g$ ,  $^4T_{1g}$ ,  $^4T_{2g}$  and a number of doublet states of which  $^6A_{1g}$  lies lowest according to Hund's rule. The free ion levels of  $Mn^{2+}$  in the order of an energy increasing are  $^6S$ ,  $^4G$ ,  $^4P$ ,  $^4D$  and  $^4F$ . The energy levels of  $Mn^{2+}$

ion in octahedral environment (CN=6) are  ${}^6A_{1g}({}^6S)$ ,  ${}^4T_{1g}({}^4G)$ ,  ${}^4T_{2g}({}^4G)$ ,  ${}^4E_g - {}^4A_{1g}({}^4G)$ ,  ${}^4T_{2g}({}^4D)$  and  ${}^4E_g({}^4D)$ . The  ${}^4E_g - {}^4A_{1g}({}^4G)$  and  ${}^4E_g({}^4D)$  levels have relatively less influence compared to the other levels by the crystal field. It means that the relative sharp lines could be expected in the absorption or excitation spectrum, which is the criterion for assignments of levels for  $Mn^{2+}$  ion. Since all the excited states of  $Mn^{2+}$  ion ( $3d^5$ ) will be either quartets or doublets, the optical absorption spectra of  $Mn^{2+}$  ions will have only spin forbidden transitions [9,24,25].

### Cobalt

Cobalt ( $d^7$ ) is divalent ion having free ion states  ${}^4F$ ,  ${}^4P$ ,  ${}^2P$ ,  ${}^2D$ ,  ${}^2G$ ,  ${}^2H$ , and  ${}^2F$  in octahedral or tetrahedral coordination. In octahedral co-ordination,  $Co^{2+}$  free ion ground state  ${}^4F$  splits into two triplets  ${}^4T_{1g}$ ,  ${}^4T_{2g}$  and a singlet  ${}^4A_{2g}$  states, while the next lowest free ion state  ${}^4P$  remains up-split with the  ${}^4T_{1g}$  state as the lowest. With regards to  $Co^{2+}$ , this co-ordination has three bands which correspond to the spin allowed transitions  ${}^4T_{1g}(F) \rightarrow {}^4T_{2g}(F)$ ,  ${}^4T_{1g}(F) \rightarrow {}^4A_{2g}(F)$  and  ${}^4T_{1g}(F) \rightarrow {}^4T_{1g}(P)$ . The  ${}^4T_{1g}(F) \rightarrow {}^4A_{2g}(F)$  transition could be seen in a low intensity due to a forbidden two-electron jump [9, 26]. In a tetrahedral symmetry, the energy levels of  $Co^{2+}$  ion are  ${}^4T_{2g}({}^4F)$ ,  ${}^4T_{1g}({}^4F)$ ,  ${}^2E_{2g}({}^2G)$  and  ${}^4T_{1g}({}^4P)$ , etc., with the ground state of  ${}^4A_{2g}({}^4F)$ . In a tetrahedral symmetry,  $Co^{2+}$  ion-doped materials mainly show two spin-forbidden transitions  ${}^4A_{2g}({}^4F) \rightarrow {}^4T_{1g}({}^4P)$  and  ${}^4A_{2g}({}^4F) \rightarrow {}^4T_{1g}({}^4F)$ , respectively [12, 26]. The high intensity of the tetrahedrally co-ordinated band is a consequence of the mixing of the 3d-orbitals with 4p-orbitals and ligand orbitals [27, 28].

## IV. Results And Discussion

### 4.1 Absorption and Photoluminescence Spectral Analysis

The absorption spectra of transition metal ions are influenced by the nature of the host matrices into which those ions are accommodated owing to the excitation spectra of 3d electrons. The absorption spectra of transition metal ions are fairly broader and are sensitive to the changes in coordination and symmetry. Due to the presence of various oxidation states, each of the states can give rise to different absorption spectra which can be explained by the application of ligand field theory. **Fig. 2 (a)** represents the absorption spectrum for reference BZM glass. From the optical absorption spectrum, it is observed that the reference glass possess UV transmission ability and good transparency.

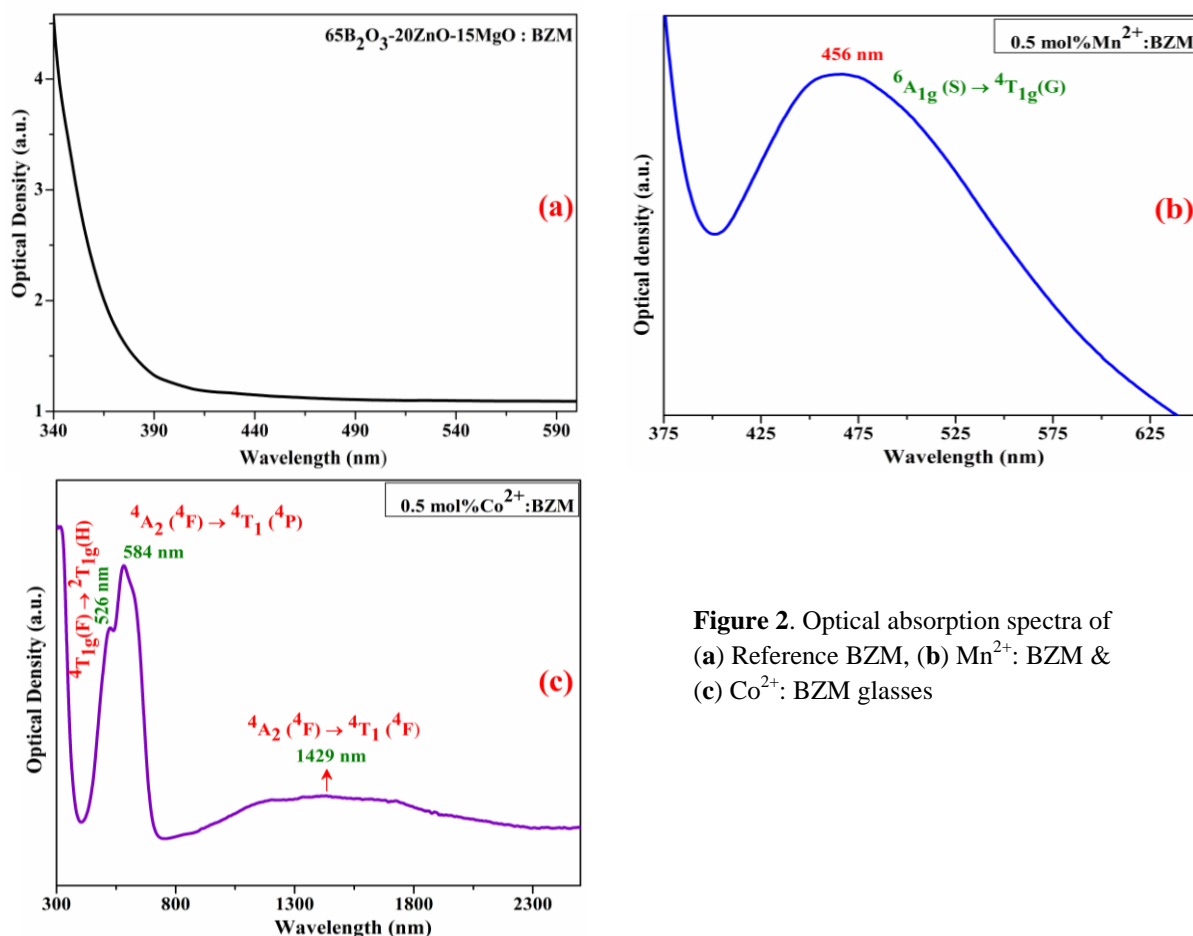


**Figure 2.** Optical absorption spectra of (a) Reference BZM, (b)  $Mn^{2+}$ : BZM & (c)  $Co^{2+}$ : BZM glasses

The visible absorption spectrum of  $Mn^{2+}$ : BZM glass is shown in **Fig. 2 (b)**, which exhibits an intense broad absorption band with the maximum centered at 456 nm assigned to the  ${}^6A_{1g}(S) \rightarrow {}^4T_{1g}(G)$  transition of  $Mn^{2+}$  ions in octahedral symmetry [7, 29]. These transitions are spin and parity forbidden for electric dipole radiation in an octahedral environment; hence the absorption bands are weak. By using the energy of this band, the crystal field parameter ( $Dq=v/10$ ) is evaluated to be  $2193\text{ cm}^{-1}$  [30].

**Fig. 2 (c)** presents the optical absorption spectrum of  $Co^{2+}$ : BZM glass recorded at room temperature in the wavelength range 300-2500 nm. The spectrum exhibited three principal absorption bands at 526 nm, 584 nm and in the NIR region at about 1429 nm. Out of these bands, the band at 526 nm is identified as being due to  ${}^4T_{1g}(F) \rightarrow {}^2T_{1g}(H)$  octahedral transition, whereas the other bands at 584 nm and 1429 nm are attributed to  ${}^4A_2({}^4F) \rightarrow {}^4T_1({}^4P)$  and  ${}^4A_2({}^4F) \rightarrow {}^4T_1({}^4F)$  tetrahedral transitions, respectively, of  $Co^{2+}$  ions [13, 31, 32]. The values of  $Dq = (v_2-v_1)/10$  (crystal field parameter) and Racah coefficient B (electrostatic parameter which is a measure of the interelectronic repulsion) are calculated from the energies corresponding to the spectral transitions using Tanabe – Sugano equation [33]. The  $Dq$  value is evaluated to be  $824\text{ cm}^{-1}$  and B is found to be  $761\text{ cm}^{-1}$  whereas C value is estimated to be  $3769\text{ cm}^{-1}$  for  $C/B = 4.5$  [33].

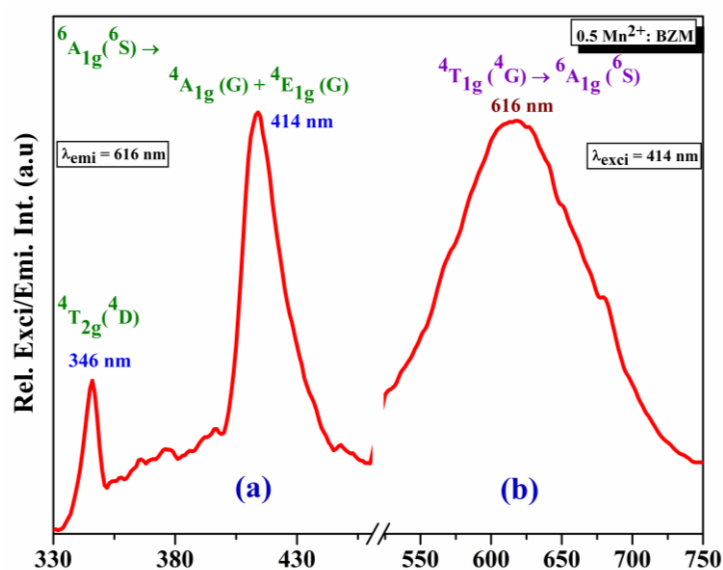


**Figure 3.** (a) Excitation and (b) Emission spectra  $Mn^{2+}$ : BZM glass

**Fig. 3(a)** shows the excitation spectrum of 0.5 mol%  $Mn^{2+}$ -doped  $65B_2O_3$ - $20ZnO$ - $15MgO$  glass. The  $Mn^{2+}$  d-d absorption transitions are difficult to be pumped as those are forbidden by spin and parity for electric dipole radiation in octahedral symmetry. Charge transfer (CT) transitions occur when a valence electron is transferred from the ligand towards the unoccupied orbitals of the metallic cation and those are parity allowed and occur generally in the UV and vacuum UV region, which are mainly vibronic in character [34]. Excitation spectrum was monitored at an emission wavelength of  $\lambda_{emi} = 616\text{ nm}$ . Two sharp excitation bands at 346 nm and at 414 nm have been measured. The excitation band at 346 nm is assigned to the  ${}^6A_{1g}({}^6S) \rightarrow {}^4T_{2g}({}^4D)$  absorption transitions of  $Mn^{2+}$  ion which exists in the UV region in absorption spectrum. Similarly, the 414 nm excitation band coincides with the energy of  ${}^6A_{1g}({}^6S) \rightarrow {}^4T_{1g}({}^4G)$  and  ${}^4E({}^4G)$  absorption transition of  $Mn^{2+}$  ion [34, 35]. Under an UV source  $Mn^{2+}$ : glasses usually emit a green or a red colour. The emission colour is strongly dependent on the co-ordination environment of  $Mn^{2+}$  in the host matrix, and it emits a green light when it is tetrahedrally co-ordinated (CN = 4), whereas it emits red in octahedral co-ordination (CN = 6). The emission spectrum of  $Mn^{2+}$ : BZM glass is shown in **Fig. 3(b)** under the excitation wavelength of 414 nm. A broad red band at 616 nm is observed and this is assigned to the spin forbidden  ${}^4T_{1g}({}^4G) \rightarrow {}^6A_{1g}({}^6S)$  transition of isolated  $Mn^{2+}$  ions in octahedral symmetry [21, 36, 37]. According to Tanabe–Sugano diagram for  $3d^5$  ions with a decreasing crystal field strength, a blue shift of the  ${}^4T_1$ - ${}^6A_1$  optical transition could be possible [38, 39]

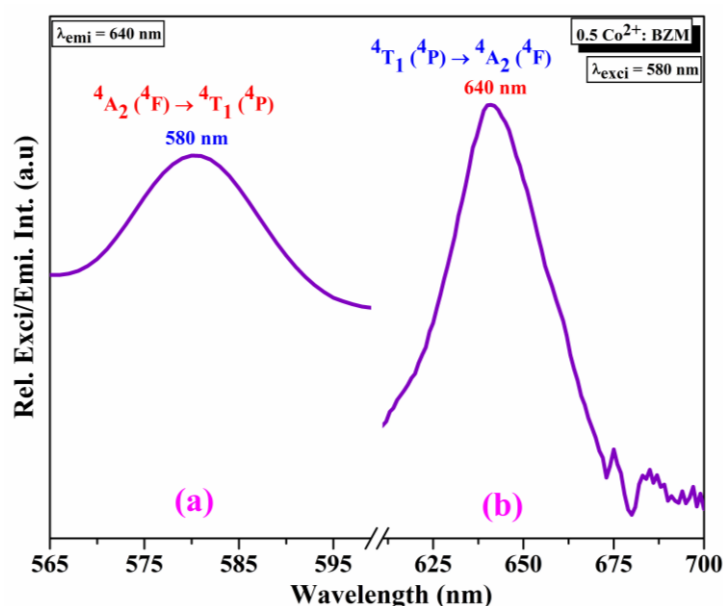


**Figure 4.** (a) Excitation and (b) Emission spectra  $Co^{2+}$ : BZM glass

The excitation spectrum of 0.2 mol%  $Co^{2+}$ : BZM glass is shown in **Fig. 4(a)**, with an emission at  $\lambda_{emi} = 640$  nm. A broad excitation peak at 580 nm ( ${}^4A_2({}^4F) \rightarrow {}^4T_1({}^4P)$ ) has been obtained. **Fig 4(b)** shows luminescence emission spectrum of  $Co^{2+}$ -doped BZM glass recorded at room temperature at an excitation wavelength of 580 nm. The spectrum exhibited a single emission band at 640 nm identified due to  ${}^4T_1({}^4P) \rightarrow {}^4A_2({}^4F)$  tetrahedral transitions of  $Co^{2+}$  ion [40, 41]. The spectral position of emission band explains about the site symmetry of  $Co^{2+}$  ion.

#### 4.2 Dielectric and Conductivity properties

The dielectric properties of glass materials are an intrinsic effect associated to the mechanism of polarization of the permanent and induced electrically charges by an external applied electric field. The charge carriers in the glass cannot move freely through a glass matrix by they can be displaced and polarized as response to an applied alternating field. In the dielectric studies, the complex permittivity of the system is calculated using the impedance data

$$\varepsilon^* = \frac{1}{(j\omega C_o Z^*)} = \varepsilon' - j\varepsilon'' \quad \dots (1)$$

Where  $Z^*$  is the complex impedance,  $C_o$  is the capacitance of free medium. The real part of permittivity (dielectric constant)  $\varepsilon'$  represents the polarizability, while the imaginary part (dielectric loss)  $\varepsilon''$  represents the energy loss due to polarization and ionic conduction. The dielectric parameters (dielectric constant ( $\varepsilon'$ ), dielectric loss tangent ( $\tan \delta$ )) and ac conductivities ( $\sigma_{ac}$ ) are calculated using the formulae [42]

$$\varepsilon' = \frac{Cd}{\varepsilon_o A} \quad \dots(2)$$

$$\tan \delta = \frac{\varepsilon''}{\varepsilon'} \quad \dots(3)$$

$$\sigma_{ac} = \omega \varepsilon_o \varepsilon'' \quad \dots(4)$$

Where  $C$  is the capacitance of the sample,  $\varepsilon_o$  is the permittivity of the free space ( $8.85 \times 10^{-12}$  F/m) and  $A$  is the cross-sectional area of electrode

The variation of dielectric constant ( $\varepsilon'$ ) at room temperature in the frequency range 1 Hz – 2 MHz for host BZM,  $Mn^{2+}$ :BZM and  $Co^{2+}$ :BZM glasses are shown in **Fig. 5(a)**. All three profiles have exhibited the same trend of rapid decreases in dielectric constant with an increase in the frequency and finally reaching a constant value.

At low frequencies, the ions align themselves along the field direction and fully contribute to the total polarization and hence high dielectric constant. As the frequency increases, the polarizability contribution from ionic and orientation sources decreases and finally disappears due to the inertia of the ions [42]. Hence, the ions would not be able to follow the electric field direction and as a result their contribution to the polarization would be less. Therefore, the dielectric constant decreases with increasing frequency. The dielectric loss tangent ( $\tan \delta$ ) is the phase difference due to the loss of energy within the sample. The contribution to the dielectric loss is mainly attributed to thermally activated relaxation of freely rotating dipoles trying to align themselves in the applied field direction.

The variation of dielectric loss tangent ( $\tan \delta$ ) with frequency at room temperature for the host BZM,  $Mn^{2+}$ : BZM and  $Co^{2+}$ : BZM glasses are shown in Fig. 5(b). From figure it is observed that dielectric loss of the three studied glass systems decreases with an increase in frequency due to mobility of conducting species. The higher the mobility of conducting species, the higher would be the dielectric loss component [43].

The frequency ( $\log \omega$ ) dependent ac conductivity ( $\log \sigma_{ac}$ ) profiles of host (BZM),  $Mn^{2+}$ :BZM and  $Co^{2+}$ : BZM glasses are shown in Fig. 6 are analyzed on the basis of Jonscher universal power law [44]:

$$\sigma(\omega) = \sigma_{dc} + A\omega^s \quad 0 < s < 1 \quad \dots (5)$$

Where  $\sigma_{dc}$  is the dc conductivity of the samples, A is temperature dependent constant,  $\omega = 2\pi f$  is the angular frequency of the applied field and s is the power law exponent in the range  $0 < s < 1$ , represents the degree of interaction between the mobile ions. The frequency dependence of conductivity is sum of dc conductivity due to movements of free charges and polarization conductivity (ac conductivity) due to movement of bound charges.

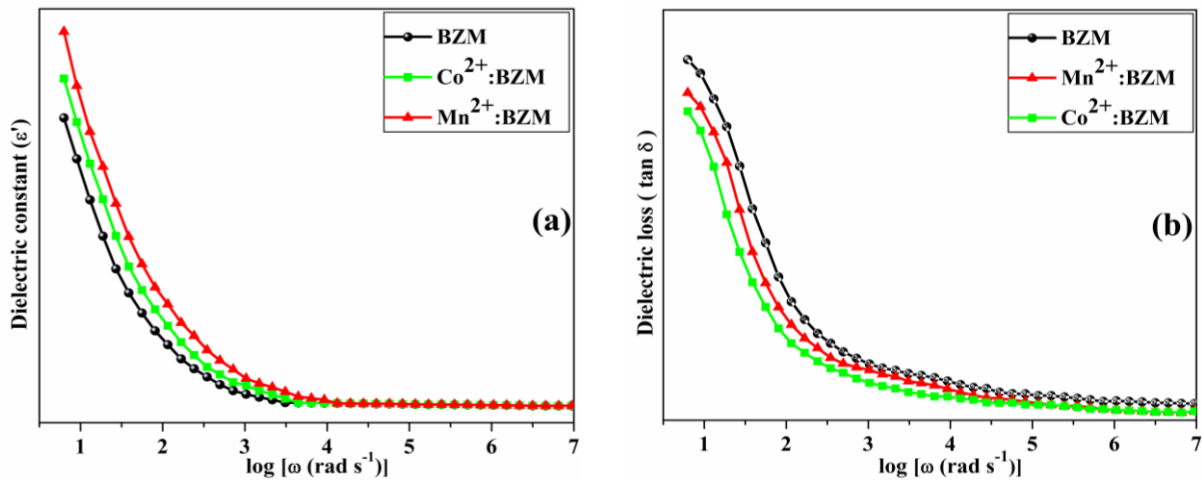


Figure 5. (a) Variation of dielectric constant ( $\epsilon'$ ) and (b) variation of loss tangent ( $\tan \delta$ ) as function of  $\log(\omega)$  at room temperature for host BZM,  $Mn^{2+}$ :BZM and  $Co^{2+}$ :BZM glasses

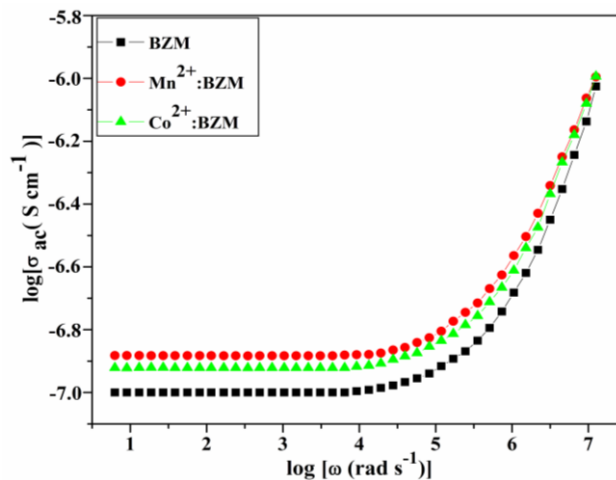


Figure 6. Variation ac conductivity  $\sigma_{ac}(\omega)$  as function of  $\log(\omega)$  at room temperature for host BZM,  $Mn^{2+}$ :BZM and  $Co^{2+}$ : BZM glasses

In **Fig. 6** profiles of frequency dependence of ac conductivity have been shown. It is observed that all the three plots have shown same trend with nearly flat portion at lower frequencies and tends to merge at higher frequencies, suggesting that at lower frequencies, conductivity is independent of the frequency and increase linearly as a function of higher frequencies. This attributes to the number of charge carriers having high relaxation time responds less due to high energy barrier in the low frequency region, so conductivity is small at lower frequencies [45]. However, due to high frequency the energy barrier height decreases and more number of charge carriers respond easily and posses short-range ion migration due to short time periods available, so higher conductivity is dominant at higher frequencies. The other possible way of explanation attributed to enhancement in ac conductivity: at lower frequencies, random distribution of ionic charges via activated hopping gives rise to a frequency independent conductivity while at higher frequencies, conductivity exhibits dispersion which increases linearly following power law relation in the higher frequency region ( $\sigma_{dc} = 0$ ) :

$$\sigma(\omega) = A\omega^s \quad 0 < s < 1 \quad \dots (6)$$

The values of the exponent  $s$  are evaluated from the slopes of  $\log \sigma_{ac}(\omega)$  versus  $\log \omega$  by using the equation

$$S = \frac{d(\ln \sigma_{ac}(\omega))}{d(\ln(\omega))}, \text{ found to lie in the range of 0.7 to 0.9 which explains the interaction between the mobile}$$

ions [46].

## V. Conclusion

In summary, it is concluded that we have developed brightly colored and transparent  $Mn^{2+}$  and  $Co^{2+}$  ions doped Borate Zinc Magnesium glasses. Vis-NIR absorption spectra of these glasses have been analyzed systematically. From  $Mn^{2+}$  ion doped BZM glass related emission spectra, it has been found that at  $\lambda_{exci} = 414$  nm, a bright red emission (616nm) ( ${}^4T_{1g}({}^4G) \rightarrow {}^6A_{1g}({}^6S)$ ) has been observed. The  $Co^{2+}$ : BZM glass has revealed a red emission (640nm) ( ${}^4T_1({}^4P) \rightarrow {}^4A_2({}^4F)$ ) at  $\lambda_{exci} = 580$  nm, and which clearly indicates that in the present host glass matrix,  $Co^{2+}$  ions are situated in tetrahedral co-ordination. These  $Mn^{2+}$  and  $Co^{2+}$  ions doped glasses have demonstrated their potential as novel luminescent optical materials of technological importance. The dielectric properties ( $\epsilon'$  &  $\tan\delta$ ) of these glasses are found to be decreasing with an increase in frequency due to accumulation of charges at the electrode-electrolyte interface hence results in with polarization effect. Due to the adding of transition metal ions ( $Mn^{2+}$  or  $Co^{2+}$ ) into the chosen host glass matrix, their ac ( $\sigma_{ac}$ ) conductivities are found to be significantly enhanced in comparison with the host (BZM) glass. Thus, we suggest that the present study has provided us progressive outlook tend in carrying out further exploration on these glasses to dope them with several other transition metal ions as dopants to evaluate their optical, dielectric and conductivity performances for applications purpose.

## References

- [1]. H. Hirashima, Y. Watamate, T. Yohida, Switching of  $TiO_2$ - $V_2O_5$ - $P_2O_5$  glasses, *J. Non-Cryst. Solids*. **95/96** (1987) 825-832.
- [2]. S. Nakamura, N. Ichinose, Study on amorphous ferrite  $CaO$ - $Bi_2O_3$ - $Fe_2O_3$  system, *J. Non-Cryst. Solids*. **95/96** (1987) 849-855.
- [3]. N.J. Kreidl, Recent applications of glass science, *J. Non-Cryst. Solids*. **123** (1990) 377-384.
- [4]. R.P. Sreekanth Chakradhar , G. Sivaramaiah, J. Lakshmana Rao, N.O. Gopal, EPR and optical investigations of manganese ions in alkali lead tetraborate glasses *Spectrochimica Acta Part A*. **62** (2005) 761-768.
- [5]. D.L. Griscom, in: L.D. Pye, V.D. Frechette, N.J. Kreidel (Eds.), *Borate Glasses: Structure, Properties and Applications*, Plenum Press, New York, 1978, p. 36
- [6]. V. Nazabal, E. Fargin, B. Ferreira, G. Le Flem, B. Desbat, T. Buffeteau, M. Couzi, V. Rodriguez, S. Santran, L. Canioni, L. Sarger, Thermally poled new borate glasses for second harmonic generation, *J. Non-Cryst. Solids*. **290** (2001)73-85.
- [7]. Shiv Prakash Singh , R.P.S.Chakradhar , J.L.Rao , Basudeb Karmakar, EPR, ptical absorption and photoluminescence properties of  $MnO_2$  doped  $23B_2O_3$ - $5ZnO$ - $72Bi_2O_3$  glasses, *Physica B*. **405** (2010) 2157-2161.
- [8]. M. Srinivasa Reddy, G. Murali Krishna, N. Veeraiah, Spectroscopic and magnetic studies of manganese ions in  $ZnO$ - $Sb_2O_3$ - $B_2O_3$  glass system, *J. Phys. Chem. Solids*. **67** (2006) 789-795.
- [9]. A. Thulasiramudu, S. Buddhudu, Optical characterization of  $Mn^{2+}$ ,  $Ni^{2+}$  and  $Co^{2+}$  ions doped zinc lead borate glasses, *J. Quant. Spectrosc. & Radiat. Transf.* **102** (2006) 212-227.
- [10]. G. Sivaramaiah, J. LakshmanaRao, Electron Spin Resonance and optical absorption spectroscopic studies of manganese centers in aluminium lead borate glasses, *Spectrochimica Acta Part A*. **98** (2012) 105-109
- [11]. B. Hemalatha Rudramadevi and S. Buddhudu, Spectral properties of  $Cu^{2+}$ ,  $Mn^{2+}$ ,  $o^{2+}$ ,  $Ni^{2+}$  &  $Cr^{3+}$  ions doped  $B_2O_3$ - $BaO$ - $LiF$  glasses, *Ferroelectric Letters Section*. **36** (3-4) (2009) 82-91.
- [12]. A. Terczynska-Madej, K. Cholewa-Kowalska, M. Laczka, Coordination and valence state of transition metal ions in alkali-borate glasses, *Optical Materials*. **33** (2011) 1984-1988.
- [13]. P. Naresh, G. Nagaraju, Ch. Srinivasa Rao, S.V.G.V.A. Prasad, V. Ravi Kumar, N. Veeraiah, Influence of ligand coordination of cobalt ions on structural properties of  $ZnO$ - $ZnF_2$ - $B_2O_3$  glass system by means of spectroscopic studies, *Physica B*. **407** (2012) 712-718.
- [14]. A. Rupesh Kumar, T.G.V.M. Rao, N. Veeraiah, M. Rami Reddy, Fluorescence spectroscopic studies of  $Mn^{2+}$  ions in  $SrO$ - $Al_2O_3$ - $B_2O_3$ - $SiO_2$  glass system, *Optical Materials*. **35** (2013) 402-406.
- [15]. H.F. Shermer, Thermal expansion of binary alkaline-earth borate glasses *J. Res. Natl. Bur. Stand. (US)* **56** (2) (1956) 73-79.

- [16]. K. Aida, T. Komastu and V. Dimitrov, Thermal stability, electronic polarisability and optical basicity of ternary tellurite glasses. *Phys. Chem. Glass.* **42** (2) (2001), 103-111.
- [17]. N. Kiran, C. R. Kesavulu, A. Suresh Kumar, J.L. Rao, Spectral studies on  $Mn^{2+}$  ions doped in sodium–lead borophosphate glasses, *Physica B.* **406** (2011) 3816-3820.
- [18]. A. Van Die, A.C.H.I. Leenaers, G. Blasse, W.F. Van Der Weg, Germanate glasses as hosts for luminescence of  $Mn^{2+}$  and  $Cr^{3+}$ , *J. Non-Cryst. Solids.* **99** (1988) 32-44.
- [19]. I. Ardelean, M. Peteanu, I. Todor, EPR and magnetic susceptibility investigation of  $MnO$ - $Bi_2O_3$  glasses, *Phys. Chem. Glasses.* **43** (2002) 276-279.
- [20]. M.L. Ovecoglu, G. Ozen, S. Cenk, Micro-structural characterization and crystallization behavior of  $(1-x)TeO_2-xWO_3$  ( $x = 0.15, 0.25, 0.3$  mol) glasses *J. Eur. Ceram. Soc.* **26** (2006) 1149-1158.
- [21]. Gandham Lakshminarayana, Lothar Wondraczek, Photoluminescence and energy transfer in  $Tb^{3+}/Mn^{2+}$  co-doped  $ZnAl_2O_4$  glass ceramics, *Journal of Solid State Chemistry.* **184** (2011) 1931–1938.
- [22]. N. Srinivasa Rao, L. Srinivasa Rao, Ch. Srinivasa Rao, B.V. Raghavaiah, V. Ravi Kumar, M.G. Brik, N. Veeraiah, Influence of valence states and co-ordination of cobalt ions on dielectric properties of  $PbO$ - $Bi_2O_3$ - $As_2O_3$ :  $CoO$  glass system, *Physica B.* **407** (2012) 581-588.
- [23]. K.H. Mahmoud, F.M. Abdel-Rahim, K. Atef, Y.B. Saddeek, Dielectric dispersion in lithium–bismuth-borate glasses, *Current Applied Physics.* **11** (2011) 55-60.
- [24]. R.P. Sreekanth Chakradhar, K.P. Ramesh, J.L.Rao, J. Ramakrishna, Mixed alkali effect in borate glass—EPR and optical absorption studies in  $xNa_2O-(30-x)K_2O-70B_2O_3$  glasses doped with  $Mn^{2+}$ , *J. Phys. Chem. Solids.* **64** (2003) 641-650.
- [25]. J. Wang, S.Wang, Q.Su, The role of excess  $Zn^{2+}$  ions in improvement of red long lasting Phosphorescence (LLP) performance of  $\beta-Zn_3(PO_4)_2:Mn$  phosphor, *J Solid State Chem.* **177** (2004) 895–900.
- [26]. G. Lakshminarayana, S. Buddhudu, Spectral analysis of  $Mn^{2+}$ ,  $Co^{2+}$  and  $Ni^{2+}$ :  $B_2O_3$ - $ZnO$ - $PbO$  glasses, *Spectrochimica Acta Part A.* **63** (2006) 295–304.
- [27]. W. Ryba-Romanowski, S. Golab, G. Dominiak-Dzik, M. Berkowski, Optical spectra of a  $LaGaO_3$  crystal singly doped with chromium, vanadium and cobalt, *J Alloys Compd.* **288** (1999) 262–268.
- [28]. X. Duan, D. Yuan, X. Cheng, Z. Sun, H. Sun, D. Xu, Mengkai Lv, Spectroscopy properties of  $Co^{2+}$ : $ZnAl_2O_4$  nanocrystals in sol-gel derived glass-ceramics, *J Phys Chem Solids* **64** (2003) 1021–1025.
- [29]. D.K. Durga, N. Veeraiah, Role of manganese ions on the stability of  $ZnF_2$ - $P_2O_5$ - $TeO_2$  glass system by the study of dielectric dispersion and some other physical properties, *J. Phys. Chem. Solids.* **64** (2003) 133–146.
- [30]. Yu-Sheng Dou, Equations for calculating  $D_q$  and  $B$ , *J. Chem. Edu.* **67** (1990) 134.
- [31]. C. Nelson, H. B. White, Transition metal ions in silicate melts. IV. Cobalt in sodium silicate and related glasses, *J. Mater. Res.* **1** (1986) 130-138.
- [32]. Ch. Rajyasree, S. Bala Murali Krishna, A. Ramesh Babu, D. Krishna Rao, Structural impact of cobalt ions on  $BaBiBO_4$  glass system by means of spectroscopic and dielectric studies, *Journal of Molecular Structure.* **1033** (2013) 200–207.
- [33]. Y. Tanabe and S. Sugano, On the absorption spectra of complex ions. *J. Phys. Soc. Jpn.* **9** (1954) 753-767.
- [34]. R. Selomulya, S. Ski, K. Pita, C.H. Kam, Q.Y. Zhang, S. Buddhudu, Luminescence properties of  $Zn_2SiO_4:Mn^{2+}$  thin-films by a sol-gel process, *Mater. Sci. Eng. B* **100** (2003) 136–141.
- [35]. J. Wang, S. Wang, Q. Su., The role of excess  $Zn^{2+}$  ions in improvement of red long lasting phosphorescence (LLP) performance of  $\beta-Zn_3(PO_4)_2:Mn$  phosphor, *J Solid State Chem.* **177** (2004) 895–900.
- [36]. T. Sanada, K. Yamamoto, N. Wada, K. Kojima, Green luminescence from Mn ions in  $ZnO$ - $GeO_2$  glasses prepared by sol-gel method and their glass ceramics, *Thin Solid Films* **496** (2006) 169-173.
- [37]. N. Da, M. Peng, S. Krolkowski, L. Wondracz, Intense red photoluminescence from  $Mn^{2+}$ -doped ( $Na^+$ ;  $Zn^{2+}$ ) sulfophosphate glasses and glass ceramics as LED converters, *Opt. Express* **18** (2010) 2549-2557.
- [38]. A. Patra, G.A. Baker, S.N. Baker, Effects of dopant concentration and annealing temperature on the phosphorescence from  $Zn_2SiO_4:Mn^{2+}$  nanocrystals, *J. Lumin.* **111** (2005) 105–111.
- [39]. R. Sarkar C.S. Tiwary, P. Kumbhakar, S. Basu, A.K. Mitra, Yellow-orange light emission from  $Mn^{2+}$ -doped  $ZnS$  nanoparticles, *Physica E.* **40** (2008) 3115-3120.
- [40]. X.L. Duan, D.R. Yuan, X.F. Cheng, Z.M. Wang, Z.H. Sun, C.N. Luan, D. Xu, M.K. Lv, Absorption and photoluminescence characteristics of  $Co^{2+}$ : $MgAl_2O_4$  nanocrystals embedded in sol-gel derived  $SiO_2$ -based glass, *Optical Materials* **25** (2004) 65-69.
- [41]. G. Nagarjuna, T. Satyanarayana, Y. Gandhi, P.V.V. Satyanarayana, N. Veeraiah, Cobalt ion as a structural probe in  $PbO$ - $As_2O_3$  glass ceramics, *Solid State Communications.* **150** (2010) 9-13.
- [42]. T. Sankarappa, M. PrashantKumar, G. B. Devidas, N. Nagaraja, R. Ramakrishnareddy, AC conductivity and dielectric studies in  $V_2O_5$ - $TeO_2$  and  $V_2O_5$ - $CoO$ - $TeO_2$  glasses, *J. Mol.Struct.* **889** (2008) 308-315.
- [43]. M.D. Ingram, Ionic Conductivity in Glasses, *Phys. Chem. Glasses* **28** (1987) 215-234.
- [44]. A.K. Jonscher, The 'universal' dielectric response, *Nature* **267** (1977) 673-679.
- [45]. H.K. Patel, S.W. Martin, Fast ionic conduction in  $Na_2S+B_2S_3$  glasses: Compositional contributions to nonexponentiality in conductivity relaxation in the extreme low-alkali-metal limit, *Phys Rev.* **B 45** (1992) 10292-10300.
- [46]. M. Krishna murthy, K.S.N. Murthy, N. Veeraiah, Dielectric properties of  $NaF$ - $B_2O_3$  glasses doped with certain transition metal ions, *Bull. Mater. Sci.* **23** (2000) 285-293.